Manuscript submitted to
AIMS' Journals
Volume **X**, Number **0X**, XX **200X**

doi:10.3934/xx.xx.xx.xx

pp. **X–XX**

# AN ANISOTROPIC PERFECTLY MATCHED LAYER METHOD FOR HELMHOLTZ SCATTERING PROBLEMS WITH DISCONTINUOUS WAVE NUMBER

ZHIMING CHEN, CHAO LIANG, AND XUESHUANG XIANG

Zhiming Chen

LSEC, Institute of Computational Mathematics and Scientific/Engineering Computing
Academy of Mathematics and Systems Science
Chinese Academy of Sciences, Beijing 100190, China

Chao Liang

LSEC, Institute of Computational Mathematics and Scientific/Engineering Computing
Academy of Mathematics and Systems Science
Chinese Academy of Sciences, Beijing 100190, China

Xueshuang Xiang

LSEC, Institute of Computational Mathematics and Scientific/Engineering Computing
Academy of Mathematics and Systems Science
Chinese Academy of Sciences, Beijing 100190, China

Abstract. The anisotropic perfectly matched layer (PML) defines a continuous vector field outside a rectangle domain and performs the complex coordinate stretching along the direction of the vector field. In this paper we propose a new way of constructing the vector field which allows us to prove the exponential decay of the stretched Green function without the constraint on the thickness of the PML layer. We report numerical experiments to illustrate the competitive behavior of the proposed PML method.

1. **Introduction.** We propose and study an anisotropic perfectly matched layer (PML) method for solving Helmholtz scattering problems with discontinuous wave number

$$\Delta u + k^2(x)u = f \quad \text{in } \Omega = \mathbb{R}^2 \setminus \bar{D}, \tag{1.1}$$

$$u = g \quad \text{on } \Gamma_D, \tag{1.2}$$

$$\sqrt{r}\left(\frac{\partial u}{\partial r} - \mathbf{i}ku\right) \to 0 \quad \text{as } r = |x| \to \infty, \tag{1.3}$$

where $D \subset \mathbb{R}^2$ is a bounded domain with Lipschitz boundary $\Gamma_D$, $f \in (H^1(\Omega))'$ has the support inside $B(R_0) = \{x \in \mathbb{R}^2 : |x| \le R_0\}$ with $(H^1(\Omega))'$ being the dual space of $H^1(\Omega)$, and $g \in H^{1/2}(\Gamma_D)$. We assume the wave number $k(x)$ is positive in $\mathbb{R}^2$ and piecewise constant outside $B(R_0)$ with the interface where the wave number

2010 *Mathematics Subject Classification.* Primary: 65N30; Secondary: 78A45, 35Q60.

*Key words and phrases.* Helmholtz equation, discontinuous wave number, anisotropic PML..

The first author is supported in part by National Basic Research Project under the grant 2011CB309700 and China NSF under the grant 11021101.

jumps being a straight line extending to infinity. We remark that the results in this paper can be extended to the other boundary conditions such as Neumann or impedance boundary conditions on $\Gamma_D$.

Since the pioneering work of Bérénger [1] which proposed a PML technique for solving the Maxwell equations, various constructions of PML absorbing layers have been proposed and studied in the literatures (cf. e.g. Turkel and Yefet [20], Teixeira and Chew [18] for the reviews). Of particular importance to the development and the analysis of the PML method is the technique of complex coordinate stretching by Chew and Weedon [10]. Under the assumption that the exterior solution is composed of outgoing waves only, the basic idea of the PML technique is to surround the computational domain by a fictitious layer of finite thickness with specially designed model medium that absorbs all the waves that propagate from inside the computational domain.

The convergence of the PML method has drawn considerable attention in the literature. Lassas and Somersalo [15, 14] and Hohage et al [12] studied the acoustic scattering problems for circular and smooth PML layers. The anisotropic PML method in which the PML layer is placed outside a rectangle or cuboid domain is of considerable interest as opposed to the circular PML method because it provides greater flexibility and efficiency to solve problems involving anisotropic scatterers. The convergence of the uniaxial PML method has been considered recently in Chen and Wu [5], Kim and Pasciak [13], Bramble and Pasciak [2], and Chen and Zheng [7] for the acoustic scattering problems. It is proved in [14, 15, 12, 5, 13, 7, 2] that the PML solution convergences exponentially to the solution of the original scattering problem as the thickness of the PML tends to infinity.

In the practical applications of the PML methods, the adaptive PML method has been proposed and studied in Chen and Wu [3] for the grating problem, Chen and Liu [4] for the acoustic scattering problem, Chen and Chen [6], and Chen, Cui and Zhang [8] for Maxwell scattering problems. The main idea of the adaptive PML method is to use the posteriori error estimate to determine the PML parameters and to use the adaptive finite element methods to solve the PML equations. The adaptive PML method provides a complete numerical strategy to solve the scattering problems in the framework of finite element which produces automatically a coarse mesh size away from the fixed domain and thus makes the total computational costs insensitive to the thickness the absorbing PML layers.

The purpose of this paper is to propose a new construction of anisotropic PML methods and use the adaptive PML method to solve the problem (1.1)-(1.3) with discontinuous wave numbers. We will extend the idea in [8] for electromagnetic scattering problems. The main idea in [8] is to define a continuous vector field outside the computational domain and perform the complex coordinate stretching along the direction of the vector field. The construction of the PML method by performing the complex coordinate stretching along a continuous vector field is different from the uniaxial PML method and seems to be more suitable for scattering problems with discontinuous wave numbers, see e.g. Oskooi et al [17]. The convergence of the anisotropic PML method in [8] is proved for a special construction of the vector field outside the cuboid domain which requires the thickness of the PML layer satisfying a uniform lower bound. This constraint is removed in the new construction of the vector field in this paper which is especially desirable for elongated PML layers. We also refer to Zschiedrich et al [21] and Trenev [19] for related ideas in designing anisotropic PML method. We will extend the anisotropic

PML method developed in this paper to solve elastic wave scattering problems for which the standard uniaxial PML method has difficulties [16].

The layout of the paper is as follows. In section 2 we introduce our new anisotropic PML method for (1.1)-(1.3) using the example of constant wave number. In section 3 we consider the guideline in constructing PML complex coordinate stretching transform in order to show the convergence of the PML method. In section 4 we introduce the finite element method for solving the PML problem. In section 5 we report two numerical examples with discontinuous wave number to show the competitive behavior of our new adaptive anisotropic PML method.

2. **The anisotropic PML method.** In this section we introduce the new anisotropic PML method for Helmholtz scattering problems. Let $D$ be contained in the interior of the rectangle $B_1 = \{x \in \mathbb{R}^2 : |x_1| < L_1/2, |x_2| < L_2/2\}$ and $\Omega_1 = B_1 \setminus \bar{D}$. Let $\Gamma_1 = \partial B_1$ and $\mathbf{n}_1$ be the unit outer normal to $\Gamma_1$. The derivation of the PML equation depends crucially on the idea of complex coordinates stretching transform $\tilde{x} = F(x)$ outside $B_1$ (see e.g. Chew and Weedon [10]), where $F : \mathbb{R}^2 \setminus \bar{B}_1 \to \mathbb{C}^2$ is a complex valued function. We set in this following $F(x) = x$ in $B_1$.

Once the transform is constructed, for the solution $u$ of the scattering problem (1.1)-(1.3), we let $\tilde{u}(x) = u(\tilde{x})$. It is clear that $\tilde{u}$ satisfies

$$\tilde{\Delta}\tilde{u} + k(x)^2\tilde{u} = 0 \quad \text{in}\, \mathbb{R}^2 \setminus \bar{B}_1, \tag{2.4}$$

where $\tilde{\Delta} = \frac{\partial^2}{\partial \tilde{x}_1^2} + \frac{\partial^2}{\partial \tilde{x}_2^2}$ is the Laplace operator with respect to the stretched coordinates. The desired PML equation can be obtained by the chain rule

$$\nabla \cdot (A(x)\nabla\tilde{u}) + J(x)k(x)^2\tilde{u} = f(x) \quad \text{in}\, \mathbb{R}^2 \setminus \bar{B}_1, \tag{2.5}$$

where $A(x) = J(x)DF^{-1}(x)DF^{-T}(x)$, $J(x) = \det(DF(x))$, and $DF(x)$ is the Jacobi matrix. The equation (2.5) should be understood in the weak sense.

Let $B_2 = \{x \in \mathbb{R}^2 : |x_1| < L_1/2 + d_1, |x_2| < L_2/2 + d_2\}$ be the rectangle which contains $B_1$. The PML solution $\hat{u}$ in $\Omega_2 = B_2 \setminus \bar{D}$ is defined as the solution of the following system

$$\nabla \cdot (A(x)\nabla\hat{u}) + J(x)k(x)^2\hat{u} = f(x) \quad \text{in}\, \Omega_2, \tag{2.6}$$

$$\hat{u} = g \quad \text{on}\, \Gamma_D, \qquad \hat{u} = 0 \quad \text{on}\, \Gamma_2. \tag{2.7}$$

The convergence of the PML solution $\hat{u}$ to the solution $u$ of the original scattering problem depends on the properties of the transform $F(x)$ to be studied in the next section.

Now we introduce a new construction of the anisotropic PML complex coordinate stretching transform $\tilde{x} = F(x)$ when the wave number $k(x)$ is a constant $k > 0$. This construction can be easily extended to the general case of piecewise constant wave numbers as shown in section 5. Let $\theta = \arctan(d_1/d_2)$. Let the domain $\Omega_{\text{PML}} = B_2 \setminus \bar{B}_1$ be divided into four trapezoids $U_i^{\pm}$, $i = 1, 2$, where

$$U_1^{\pm} = \{x \in \mathbb{R}^2 : \frac{L_1}{2} \le \pm x_1 \le d_1 + \frac{L_1}{2},\ |x_2| \le \frac{L_2}{2} + \big(|x_1| - \frac{L_1}{2}\big)\tan\theta\},$$

$$U_2^{\pm} = \{x \in \mathbb{R}^2 : \frac{L_2}{2} \le \pm x_2 \le d_2 + \frac{L_2}{2},\ |x_1| \le \frac{L_1}{2} + \big(|x_2| - \frac{L_2}{2}\big)\cot\theta\}.$$

In each domain $U_i^{\pm}$, $i = 1, 2$, we write the Cartesian coordinate $x = (x_1, x_2)$ in a new coordinate $(r, s)$ so that the PML coordinate stretching is performed only in one direction outside $B_1$. We will only describe the construction in $U_1^+$ and $U_2^+$. The other domains can be considered similarly.

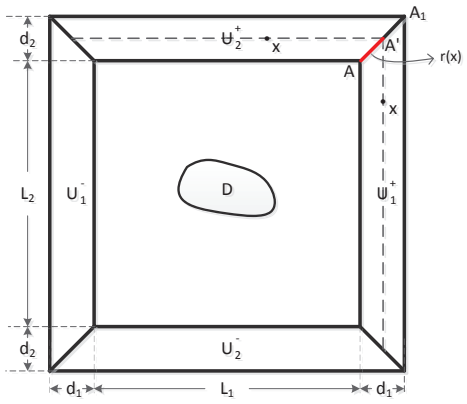


FIGURE 2.1. *Setting of the scattering problem with the PML layer.*

For $x \in U_1^+$, we define $r \in (0, \sqrt{d_1^2 + d_2^2}), s \in [-1, 1]$ such that

$$x_1 = \frac{L_1}{2} + r\cos\theta, \tag{2.8}$$

$$x_2 = \begin{cases} \mathrm{sgn}(x_2)\frac{L_2}{2} + r\sin\theta \cdot s & L_2/2 \le |x_2| \le L_2/2 + d_2, \\ x_2 & |x_2| \le L_2/2. \end{cases} \tag{2.9}$$

We know that $r = r(x) = \frac{x_1 - L_1/2}{\cos\theta}$ which is the distance between $A$ and $A' = (x_1, \frac{L_2}{2} + \frac{d_2}{d_1}(x_1 - \frac{L_1}{2}))$ on the segment $AA_1$ (see Fig. 2.1).

For $x \in U_2^+$, we define $r \in (0, \sqrt{d_1^2 + d_2^2}), s \in [-1, 1]$ such that

$$x_1 = \begin{cases} \mathrm{sgn}(x_1)\frac{L_1}{2} + r\cos\theta \cdot s & L_1/2 \le |x_1| \le L_1/2 + d_1, \\ x_1 & |x_1| \le L_1/2, \end{cases} \tag{2.10}$$

$$x_2 = \frac{L_2}{2} + r\sin\theta. \tag{2.11}$$

We know that $r = r(x) = \frac{x_2 - L_2/2}{\sin\theta}$ which is the distance between $A$ and $A' = (\frac{L_1}{2} + \frac{d_1}{d_2}(x_2 - \frac{L_2}{2}), x_2)$ on the segment $AA_1$ (see Fig. 2.1). Obviously $r(x)$ is continuous in $\Omega_{\mathrm{PML}}$.

Now we define the complex coordinate stretching. For $t > 0$, let

$$\alpha(t) = \eta(t) + \mathbf{i}\sigma(t), \quad \eta(t) = 1 + \zeta\sigma(t),$$

be the model medium property, where $\zeta \ge 0$ is a constant and $\sigma(t) > 0$ for $t > 0$ and $\sigma(0) = 0$. Denote $\tilde{r}(x)$ as the complex stretching of $r(x)$

$$\tilde{r}(x) := \int_0^{r(x)} \alpha(t)\,\mathrm{d}t = r(x) + (\zeta + \mathbf{i})\int_0^{r(x)} \sigma(t)\,\mathrm{d}t$$

and define the complex coordinates $(\tilde{x}_1, \tilde{x}_2)$ for $x \in U_1^+$ as

$$\tilde{x}_1 = \frac{L_1}{2} + \tilde{r}(x)\cos\theta,$$

$$\tilde{x}_2 = \begin{cases} \mathrm{sgn}(x_2)\frac{L_2}{2} + \tilde{r}(x)\sin\theta \cdot s & L_2/2 \le |x_2| \le L_2/2 + d_2, \\ x_2 & |x_2| \le L_2/2. \end{cases}$$

By using (2.8)-(2.9) we know that, for $x \in U_1^+$,

$$\tilde{x}_1 = \frac{L_1}{2} + \beta(r(x))(x_1 - \frac{L_1}{2}), \tag{2.12}$$

$$\tilde{x}_2 = \begin{cases} \mathrm{sgn}(x_2)\frac{L_2}{2} + \beta(r(x))(x_2 - \mathrm{sgn}(x_2)\frac{L_2}{2}) & L_2/2 \le |x_2| \le L_2/2 + d_2, \\ x_2 & |x_2| \le L_2/2, \end{cases} \tag{2.13}$$

where $\beta(r(x)) = \hat{\eta}(r(x)) + \mathbf{i}\hat{\sigma}(r(x))$, $\hat{\eta}(r(x)) = 1 + \zeta\hat{\sigma}(r(x))$, and $\hat{\sigma}(t) = \frac{1}{t}\int_0^t \sigma(s)\,\mathrm{d}s$. (2.12)-(2.13) defines the desired complex coordinate stretching transform $F(x)$ in $U_1^+$.

To conclude this section, for the sake of later reference, we write down the explicit formula for the matrix $A$ in the domain $U_1^+$. The formulas in other domains are similar. For $x \in U_1^+$, it is easy to check that when $|x_2| > L_2/2$,

$$DF = \begin{pmatrix} \alpha & 0 \\ (\alpha - \beta)\tan\theta \cdot s & \beta \end{pmatrix}, \quad A = \begin{pmatrix} \frac{\beta}{\alpha} & -\frac{\alpha-\beta}{\alpha}\tan\theta \cdot s \\ -\frac{\alpha-\beta}{\alpha}\tan\theta \cdot s & \frac{(\alpha-\beta)^2}{\alpha\beta}\tan^2\theta \cdot s^2 + \frac{\alpha}{\beta} \end{pmatrix},$$

and when $|x_2| \le L_2/2$,

$$DF = \begin{pmatrix} \alpha & 0 \\ 0 & 1 \end{pmatrix}, \quad A = \begin{pmatrix} \alpha^{-1} & 0 \\ 0 & \alpha \end{pmatrix}.$$

Here $\alpha = \alpha(r(x))$ and $\beta = \beta(r(x))$.

## 3. The complex coordinates stretching transform.

In this section we consider the guideline in constructing the PML complex coordinate stretching transform $\tilde{x} = F(x)$ in order to obtain the convergence of the PML method by extending the analysis in [8] for Maxwell scattering problems with constant wave number. In this section we assume the wave number $k(x)$ is constant $k$. The results can also be extended to the case of layered medium using the method developed in [7] where the uniaxial PML method is studied.

### 3.1. Ellipticity of $A(x)$.

The first important property is the ellipticity of the PML coefficient matrix $A$. We start with the following lemma which can be proved by the same method as in [8, Lemma 7].

**Lemma 3.1.** *Let $C = (c_{ij}) \in \mathbb{R}^{2\times 2}$ be a symmetric matrix such that $c_{11} + c_{22} > 0$ and $c_{11}c_{22} - c_{12}^2 \ge 0$. Then the eigenvalues of $C$ is bounded below by $\frac{c_{11}c_{22}-c_{12}^2}{c_{11}+c_{22}}$.*

We need the following assumption on the medium property

**(H1)** $\zeta \ge \max\limits_{i,j=1,2} \dfrac{d_i}{d_j}$ and $\sigma = \hat{\sigma} = \sigma_0$ for $t \ge r_0 > 0$, where $\sigma_0$ is a constant.

**Lemma 3.2.** *Let (H1) be satisfied. Then*

$$\mathrm{Re}(A(x)\xi \cdot \bar{\xi}) \ge \frac{1}{(1+\zeta^2)(1+|\alpha|)|\alpha|^2|\beta|^2}\xi \cdot \bar{\xi}.$$

*Proof.* We only prove the lemma for $x \in U_1^+$. The other cases are similar. By the formula at the end of last section, write $A(x) = (a_{ij}(x))$, we know that for any $x \in U_1^+$,

$$\mathrm{Re}(A(x)\xi \cdot \bar{\xi}) = \sum_{i,j=1}^{2} \mathrm{Re}(a_{ij}(x))\xi_i\bar{\xi}_j \ge \Big[\min_{j=1,2}\lambda_j(x)\Big](\xi \cdot \bar{\xi}),$$

where $\lambda_j(x), j = 1, 2$, are the eigenvalues of the symmetric matrix $\mathrm{Re}A(x)$.

Lemma 3.2 is obvious for $|x_2| \le L_2/2$. For $|x_2| \ge L_2/2$, it is easy to check that

$$\mathrm{Re}\,\frac{(\alpha-\beta)^2}{\alpha\beta} = \frac{(\sigma-\hat\sigma)^2}{|\alpha|^2|\beta|^2}\left[(\zeta^2-1)(\eta\hat\eta-\sigma\hat\sigma)+2\zeta(\sigma\hat\eta+\hat\sigma\eta)\right] \ge 0,$$

where we have used the fact that $\zeta \ge 1$ by (H1). Thus

$$\mathrm{Re}\,(a_{11}) + \mathrm{Re}\,(a_{22}) = \mathrm{Re}\,\frac{\beta}{\alpha} + \mathrm{Re}\,\frac{\alpha}{\beta} + \mathrm{Re}\,\frac{(\alpha-\beta)^2}{\alpha\beta}\tan^2\theta\cdot s^2 > 0.$$

On the other hand, since $\mathrm{Re}\,\frac{(\alpha-\beta)^2}{\alpha\beta} = \mathrm{Re}\,\frac{\beta}{\alpha} + \mathrm{Re}\,\frac{\alpha}{\beta} - 2$ and $\mathrm{Re}\,\frac{\alpha-\beta}{\alpha} = 1 - \mathrm{Re}\,\frac{\beta}{\alpha}$, we have

$$\begin{aligned}\mathrm{Re}(a_{11})\mathrm{Re}(a_{22}) - \mathrm{Re}(a_{12})^2 &= \mathrm{Re}\,\frac{\beta}{\alpha}\cdot\mathrm{Re}\,\frac{\alpha}{\beta} + \left(\mathrm{Re}\,\frac{\beta}{\alpha}\cdot\mathrm{Re}\,\frac{\alpha}{\beta} - 1\right)\tan^2\theta\cdot s^2\\ &= \frac{1}{|\alpha|^2|\beta|^2}\left[(\eta\hat\eta+\sigma\hat\sigma)^2 - (\hat\sigma\eta-\sigma\hat\eta)^2\tan^2\theta\cdot s^2\right].\end{aligned}$$

Since $(\hat\sigma\eta-\sigma\hat\eta)^2 = (\sigma-\hat\sigma)^2 \le \sigma^2$ and $\eta\hat\eta+\sigma\hat\sigma \ge 1+\zeta\sigma$, we know that

$$\mathrm{Re}(a_{11})\mathrm{Re}(a_{22}) - \mathrm{Re}(a_{12})^2 \ge \frac{1}{|\alpha|^2|\beta|^2}\left[(1+\zeta\sigma)^2 - \frac{d_2^2}{d_1^2}\sigma^2\right] \ge \frac{1}{|\alpha|^2|\beta|^2},$$

where we have used $s^2 \in [0,1]$ and (H1). This completes the proof by using Lemma 3.2 and the fact that $\mathrm{Re}\,(a_{11})+\mathrm{Re}\,(a_{22}) \le (1+|\alpha|)(1+d_2^2/d_1^2) \le (1+|\alpha|)(1+\zeta^2)$. □

3.2. **Exponential decay of the stretched Green function.** It is clear that any solution of the exterior Dirichlet problem (1.1)-(1.3) satisfies

$$u(x) = -\Psi_{\mathrm{SL}}(\frac{\partial u}{\partial \mathbf{n}_1})(x) + \Psi_{\mathrm{DL}}(u)(x) \quad \text{in}\,\Omega\setminus\bar B_1,$$

where $\Psi_{\mathrm{SL}}(\lambda)(x)$, $\Psi_{\mathrm{DL}}(\xi)(x)$ are, respectively, the single and double layer potentials

$$\begin{aligned}\Psi_{\mathrm{SL}}(\lambda)(x) &= \int_{\Gamma_1} G(x,y)\lambda(y)\,\mathrm{d}s(y), \quad \forall\lambda\in H^{-1/2}(\Gamma_1),\\ \Psi_{\mathrm{DL}}(\xi)(x) &= \int_{\Gamma_1}\frac{\partial G(x,y)}{\partial\mathbf{n}_1}\xi(y)\,\mathrm{d}s(y), \quad \forall\xi\in H^{-1/2}(\Gamma_1).\end{aligned}$$

Here $G(x,y) = \frac{\mathbf{i}}{4}H_0^{(1)}(k|x-y|)$ is the fundamental solution of the Helmholtz equation (1.1)-(1.2) satisfying the Sommerefeld radiation condition (1.3).

For any $z\in\mathbb{C}$, $z^{1/2}$ is taken as the analytic branch of $\sqrt{z}$ such that $\mathrm{Re}\,(z^{1/2}) > 0$ for any $z\in\mathbb{C}\setminus(-\infty,0]$. Denote $\rho(\tilde x,y) = [(\tilde x_1-y_1)^2+(\tilde x_2-y_2)^2]^{1/2}$ the complex stretched distance. Let $\tilde G(x,y) = G(\tilde x,y) = \frac{\mathbf{i}}{4}H_0^{(1)}(k\rho(\tilde x,y))$ be the stretched Green function. Then we know that

$$\tilde u = -\tilde\Psi_{\mathrm{SL}}(\frac{\partial u}{\partial\mathbf{n}_1})(x) + \tilde\Psi_{\mathrm{DL}}(u)(x) \quad \text{for}\, x\in\mathbb{R}^2\setminus\bar B_1, \tag{3.14}$$

where $\tilde\Psi_{\mathrm{SL}}(\lambda)(x), \tilde\Psi_{\mathrm{DL}}(\xi)(x)$ are the modified single and double layer potentials

$$\begin{aligned}\tilde\Psi_{\mathrm{SL}}(\lambda)(x) &= \int_{\Gamma_1}\tilde G(x,y)\lambda(y)\,\mathrm{d}s(y), \quad \forall\lambda\in H^{-1/2}(\Gamma_1),\\ \tilde\Psi_{\mathrm{DL}}(\xi)(x) &= \int_{\Gamma_1}\frac{\partial\tilde G(x,y)}{\partial\mathbf{n}_1}\xi(y)\,\mathrm{d}s(y), \quad \forall\xi\in H^{-1/2}(\Gamma_1).\end{aligned}$$

The following lemma proved in [4, Lemma 2.2] indicates that the first Hankel function decays exponentially away from the upper half complex plane.

**Lemma 3.3.** *For any* $\nu \in \mathbb{R}, z \in \mathbb{C}_{++} = \{z \in \mathbb{C} : \mathrm{Re}\,(z) \geq 0, \mathrm{Im}\,(z) \geq 0\}$, *and* $\Theta \in \mathbb{R}$ *such that* $0 < \Theta \leq |z|$, *we have*

$$|H_\nu^{(1)}(z)| \leq e^{-\mathrm{Im}\,(z)\left(1-\frac{\Theta^2}{|z|^2}\right)^{1/2}} |H_\nu^{(1)}(\Theta)|.$$

From Lemma 3.3 and (3.14) we know that to ensure the exponential decay of the stretched Green solution $\tilde{G}(x, y)$, we need a uniform lower bound of $\mathrm{Im}\,\rho(\tilde{x}, y)$ which tends to infinity when the thickness of the PML layer or the PML medium property tends to infinity. We first recall the following lemma from [5].

**Lemma 3.4.** *For any* $z_1 = a_1 + \mathbf{i}b_1, z_2 = a_2 + \mathbf{i}b_2$ *with* $a_1, b_1, a_2, b_2 \in \mathbb{R}$ *such that* $a_1b_1 + a_2b_2 > 0$, *we have*

$$\mathrm{Im}(z_1^2 + z_2^2)^{1/2} \geq \frac{a_1b_1 + a_2b_2}{\sqrt{a_1^2 + a_2^2}}.$$

**Lemma 3.5.** *Let* $z_j = \tilde{x}_j - y_j$, $j = 1, 2$. *For any* $x \in \Gamma_2$, $y \in \bar{B}_1$, *we have*

$$\mathrm{Im}\rho(\tilde{x}, y) \geq \frac{\sigma_0 \min(d_1^2, d_2^2)}{\sqrt{(L_1 + d_1)^2 + (L_2 + d_2)^2}} = \gamma_0.$$

*Proof.* We only prove the case when $x \in \Gamma_2 \cap \bar{U}_1^+$ in which case $x_1 = L_1/2 + d_1$. If $|x_2| \geq L_2/2$, we have from (2.12)-(2.13) that

$$z_1 = \tilde{x}_1 - y_1 = x_1 - y_1 + \zeta\sigma_0 \left(x_1 - \frac{L_1}{2}\right) + \mathbf{i}\sigma_0 \left(x_1 - \frac{L_1}{2}\right),$$
$$z_2 = \tilde{x}_2 - y_2 = x_2 - y_2 + \zeta\sigma_0 \left(x_2 - \mathrm{sgn}(x_2)\frac{L_2}{2}\right) + \mathbf{i}\sigma_0 \left(x_2 - \mathrm{sgn}(x_2)\frac{L_2}{2}\right).$$

It is easy to know that for $y \in \bar{B}_1$,

$$(x_1 - y_1)\left(x_1 - \frac{L_1}{2}\right) > 0, \quad (x_2 - y_2)\left(x_2 - \mathrm{sgn}(x_2)\frac{L_2}{2}\right) \geq 0.$$

Thus by Lemma 3.4 we have

$$\begin{aligned} \mathrm{Im}\rho(\tilde{x}, y) &\geq \frac{\sigma_0|x_1 - y_1||x_1 - \frac{L_1}{2}| + \zeta\sigma_0^2|x_1 - \frac{L_1}{2}|^2}{(1 + \zeta\sigma_0)|x - y|} \\ &\geq \frac{\sigma_0 d_1^2}{\sqrt{(L_1 + d_1)^2 + (L_2 + d_2)^2}}. \end{aligned} \tag{3.15}$$

The case when $|x_2| \leq L_2/2$ is simpler since $\tilde{x}_2 = x_2$. This completes the proof. □

We remark that in this lemma we do not require the thickness of the PML layer $d_1, d_2$ should have a uniform lower bound as required in [8, Lemma 3]. This is the main advantage of our new complex stretching formulation in this paper.

Based on Lemma 3.1 and Lemma 3.5, the convergence of PML solution $\hat{u}$ to the solution of (1.1)-(1.3) can be proved by the method in [8]. Here we omit the details.

## 4. Finite element approximation.

In this section we introduce the finite element approximations (2.6)-(2.7). Let $b : H^1(\Omega_2) \times H^1(\Omega_2) \to \mathbb{C}$ be the sesquilinear form given by

$$b(\varphi, \psi) = \int_{\Omega_2} (A(x)\nabla\varphi \cdot \nabla\bar{\psi} - J(x)k(x)^2\varphi\bar{\psi})\,\mathrm{d}x. \tag{4.16}$$

The weak formulation of (2.6)-(2.7) is: Given $g \in H^{1/2}(\Gamma_D)$, find $\hat{u} \in H^1(\Omega_2)$ such that $u = g$ on $\Gamma_D$, $u = 0$ on $\Gamma_2$, and

$$b(\hat{u}, \psi) = 0, \quad \forall \psi \in H_0^1(\Omega_2). \tag{4.17}$$

Let $\Gamma_D^h$ be a piecewise linear approximation of the boundary $\Gamma_D$ and $\Omega_2^h$ be the domain bounded by $\Gamma_2$ and $\Gamma_D^h$. Let $\mathcal{M}_h$ be a regular triangulation of the domain $\Omega_2^h$ such that the wave number $k(x)$ is constant on each element $K \in \mathcal{M}_h$. Let $V_h \subset H^1(\Omega_2^h)$ be the conforming linear finite element space over $\Omega_2^h$ and $\overset{\circ}{V}_h = \{v_h \in V_h : v_h = 0 \text{ on } \Gamma_D^h \cup \Gamma_2\}$. The finite element approximation to the PML problem (2.6)-(2.7) reads as follows: Find $u_h \in V_h$ such that $u_h = g_h$ on $\Gamma_D^h$, $u_h = 0$ on $\Gamma_2$, and

$$b(u_h, \psi_h) = 0, \quad \forall \psi_h \in \overset{\circ}{V}_h. \tag{4.18}$$

Here $g_h$ is some piecewise linear approximation of $g$.

We will use adaptive finite element method based on a posteriori error estimate to solve the discrete problem (4.18). We now introduce the a posteriori error estimator used in our numerical experiments in the next section. For any $K \in \mathcal{M}_h$, we denote $h_K$ its diameter. Let $\mathcal{B}_h$ denote the set of all sides that do not lie on $\Gamma_D^h$ and $\Gamma_2$. For any $e \in \mathcal{B}_h, h_e$ stands for its length. For any $K \in \mathcal{M}_h$, we define the residual

$$R_h := \nabla \cdot (A \nabla u_h\big|_K) + Jk(x)^2 u_h\big|_K. \tag{4.19}$$

For any interior side $e \in \mathcal{B}_h$ which is common side of $K_1$ and $K_2 \in \mathcal{M}_h$, we define the jump residual across $e$:

$$J_e := (A \nabla u_h\big|_{K_1} - A \nabla u_h\big|_{K_2}) \cdot \nu_e, \tag{4.20}$$

using the convention that the unit normal $\nu_e$ to $e$ points from $K_2$ to $K_1$. For any $K \in \mathcal{M}_h$, the local error estimator $\eta_K$ is then defined as

$$\eta_K = \Big( ||h_K R_h||^2_{L^2(K)} + \frac{1}{2} \sum_{e \subset \partial K} h_e ||J_e||^2_{L^2(e)} \Big)^{1/2}. \tag{4.21}$$

5. **Implementation and numerical examples.** In this section we report two numerical examples to illustrate the performance of the new anisotropic PML method in this paper. The computations are carried out in MATLAB on Dell Precision T5500 with Intel(R) Xeon(R)CPU 2.67GHz. The PML parameters are determined as follows. First we choose $L_1, L_2$ such that $D \subset B_1$. We choose the thickness of the PML layer $d_1, d_2 > 0$. We take $\zeta = \max_{i,j=1,2} d_i/d_j$ in $\eta = 1 + \zeta\sigma$ and choose the medium property $\sigma(t) = (t\hat{\sigma}(t))'$ with

$$\hat{\sigma}(t) = \sigma_0 \Big( \int_0^t s^2 (r_0 - s)^2 \, \mathrm{d}s \Big) \Big( \int_0^{r_0} s^2 (r_0 - s)^2 \, \mathrm{d}s \Big)^{-1}, \quad \forall t \in (0, r_0).$$

Let $k_{\min} = \min\{k(x) : x \in \mathbb{R}^2\}$. The constant $\sigma_0$ is so chosen that the exponentially decaying factor

$$\omega = e^{-\gamma_0 k_{\min}} = e^{-\frac{\sigma_0 \min(d_1^2, d_2^2)}{\sqrt{(L_1+d_1)^2 + (L_2+d_2)^2}} k_{\min}} \leq 10^{-8}, \tag{5.22}$$

which makes the PML error negligible compared with the finite element discretization error.

Once the PML region and the medium property are fixed, we use the standard finite element adaptive strategy to modify the mesh according to the posteriori error

estimate with the local error estimator $\eta_K$ in (4.21). We define the global posteriori error estimate

$$\mathcal{E} = \Big( \sum_{K\in\mathcal{M}_h} \eta_K^2 \Big)^{1/2}.$$

Now we introduce the adaptive anisotropic PML algorithm used in this paper.

**Algorithm 5.1.** Given tolerance TOL>0 and the initial mesh $\mathcal{M}_0$. Set $\mathcal{M}_h = \mathcal{M}_0$.
(1) Solve the discrete problem (4.18) on $\mathcal{M}_0$.
(2) Compute the local error estimator $\eta_K$ on each $K \in \mathcal{M}_0$ and the global a posteriori error estimate $\mathcal{E}$.
(4) While $\mathcal{E} >$ TOL do
• Refine elements in $\hat{\mathcal{M}}_h \subset \mathcal{M}_h$, where $\hat{\mathcal{M}}_h$ is the minimum subset of $\mathcal{M}_h$ such that

$$\Big( \sum_{K\in\hat{\mathcal{M}}_h} \eta_K \Big)^{1/2} \geq \frac{1}{2}\,\mathcal{E}.$$

• Solve the discrete problem (4.18) on $\mathcal{M}_h$.
• Computer the local error estimators $\eta_K$ on each $K \in \mathcal{M}_h$ and the global a posteriori error estimate $\mathcal{E}$.
end while

**Example 5.1.** We consider the Helmholtz problem (1.1)-(1.3) in a two layered medium where $k(x)$ is defined by

$$k(x) = \begin{cases} k_1 & \text{if } x_2 \geq x_1, \\ k_2 & \text{if } x_2 < x_1. \end{cases} \tag{5.23}$$

We note that in this example the interface where the wave number is discontinuous does not align with the coordinate axises. The fundamental solution of Helmholtz equation with this wave number can be constructed by using the method in [7] to which we refer for further details. First we introduce some notation. Let $h$ be a bounded analytical function in $\mathbb{C} \setminus ((-\infty, -k_1] \cup [k_1, \infty))$, $k_1 \leq k_2$. For any $a \in \mathbb{R}, b > 0$, we denote

$$I(h; a, b) = \frac{\mathbf{i}}{2\pi} \int_{\mathrm{SIP}} \frac{h(\xi)}{\mu_1 + \mu_2} e^{\mathbf{i}\xi a + \mathbf{i}\mu_1 b}\, \mathrm{d}\xi, \tag{5.24}$$

where SIP is the Sommerfeld integral path ([9], [7]). By [7, Lemma 2.1], $I(h; a, b)$ can be computed by the following identity

$$I(h; a, b) = \frac{\mathbf{i}}{2\pi} \int_1^\infty \frac{1}{\sqrt{t^2-1}} \Big[ \Big( \frac{\mu_1}{\mu_1+\mu_2} h \Big)(\xi) + \Big( \frac{\mu_1}{\mu_1+\mu_2} h \Big)(\bar{\xi}) \Big] e^{\mathbf{i}k_1\rho t}\, \mathrm{d}t, \tag{5.25}$$

where $\rho = \sqrt{a^2+b^2}$, $\xi = \frac{k_1|a|t}{\rho} + \mathbf{i}\frac{k_1 b\sqrt{t^2-1}}{\rho}$, and $\mu_j = (k_j^2 - \xi^2)^{1/2}$, $j = 1, 2$. Suppose the dirac source $\delta_y(x)$ is located at $y \in \{x \in \mathbb{R}^2 : x_2 \geq x_1\}$, then the fundamental solution function $G(x, y)$ is

$$G(x,y) = \begin{cases} \Phi(k_1, \bar{x}, \bar{y}) - \Phi(k_1, \bar{x}, \bar{y}') + I(1; \bar{x}_1 - \bar{y}_1, \bar{x}_2 + \bar{y}_2) & \text{if } x_2 - x_1 \geq 0, \\ I(e^{\mathbf{i}(\mu_1-\mu_2)\bar{x}_2}; \bar{x}_1 - \bar{y}_1, -\bar{x}_2 + \bar{y}_2) & \text{if } x_2 - x_1 < 0, \end{cases}$$

where $\bar{x} = (\frac{\sqrt{2}}{2}(x_1 + x_2), \frac{\sqrt{2}}{2}(x_2 - x_1))$ and $\bar{y}' = (\bar{y}_1, -\bar{y}_2)$ is the image of $\bar{y}$. Here $\Phi(k, x, y) = \frac{\mathbf{i}}{4} H_0^{(1)}(k|x-y|)$ and $H_0^{(1)}(z)$ is the first Hankel function of order zero.

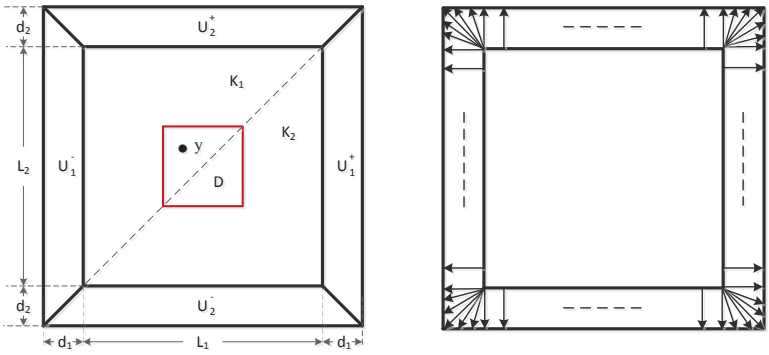


FIGURE 5.2. *The domain setting and the direction of the vector field along which the PML complex coordinate stretching is performed in Example 1.*

Based on the fundamental function $G(x, y)$, we can construct an analytic solution of the problem (1.1)-(1.3) with the scatterer $D = (-1, 1) \times (-1, 1)$. Suppose $y = (-0.5, 0.5)$. We set the source $f = 0$ and boundary condition $g = G(x, y)$ in (1.1)-(1.3). Then the exact solution of (1.1)-(1.3) is $G(x, y)$ as we defined above. We take $L_1 = L_2 = 6$ , the thickness of PML layer $d_1 = d_2 = 1$, and the wave numbers $k_1 = 3\pi$, $k_2 = 5\pi$. Figure 5.2 shows the setting of domain and the direction of the vector field along which the PML coordinate stretching is performed. We choose the PML parameters $\sigma_0 = 11.86$ and $r_0 = 0.5$ to ensure (5.22).

It is clear that the direction of the vector field is continuous across the discontinuous interface. We use the complex coordinate stretching transform in section 2 to define the anisotropic PML problem. Figure 5.3 shows the log $N_k$-log $||u - u_k||_{H^1(\Omega_1)}$ and log $N_k$-log $\mathcal{E}_k$ curves, where $N_k$ is the number of nodes of the mesh $\mathcal{M}_k$ and $u_k$ is the finite element solution over the mesh $\mathcal{M}_k$. It indicates clearly that the meshes and the associated numerical complexity are quasi-optimal: $||u - u_k||_{H^1(\Omega_1)} \approx CN_k^{-1/2}$ and $\mathcal{E}_k \approx CN_k^{-1/2}$ are valid asymptotically. As a comparison, we also show the log $N_k$-log $||u - u_k||_{H^1(\Omega_1)}$ and log $N_k$-log $\mathcal{E}_k$ curves by using adaptive uniaxial PML method. We observe that two methods perform comparably.

Figure 5.4 shows the adaptive mesh. We observe that the mesh in the domain with larger wave number is more refined. This is reasonable since it needs more DOFs to resolve the wave in the domain with larger wave number. We also show the real part of numerical and exact solutions in Figure 5.5 from two different observation directions.

**Example 5.2.** In this example, we show that our new PML method can be used to solve the scattering problems with several discontinuous interfaces. The wave number $k(x)$ is defined by

$$k(x) = \begin{cases} k_1 & \text{if } x \in D_1, \\ k_2 & \text{if } x \in D_2, \\ k_3 & \text{if } x \in D_3, \end{cases} \tag{5.26}$$

where $D_1 = \{x \in \mathbb{R}^2 : -x_1 - 2 \le x_2 \le 0.6(x_1 + 2)\}$, $D_2 = \{x \in \mathbb{R}^2 : x_2 \le 0, x_2 \le -x_1 - 2\}$, and $D_3 = \{x \in \mathbb{R}^2 : x_2 > 0, x_2 \ge 0.6(x_1 + 2)\}$. We take $k_1 = 4\pi$,

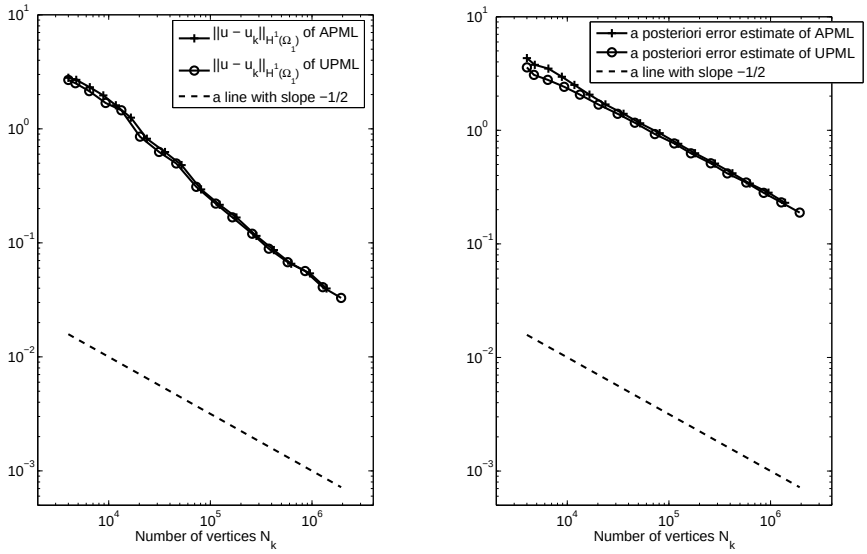


(a) (b)

FIGURE 5.3. *(a) The quasi-optimality of the adaptive mesh refinements of the error* $||u-u_k||_{H^1(\Omega_1)}$ *for Example 1; (b) The quasi-optimality of the adaptive mesh refinements of the a posteriori error estimate for Example 1.*

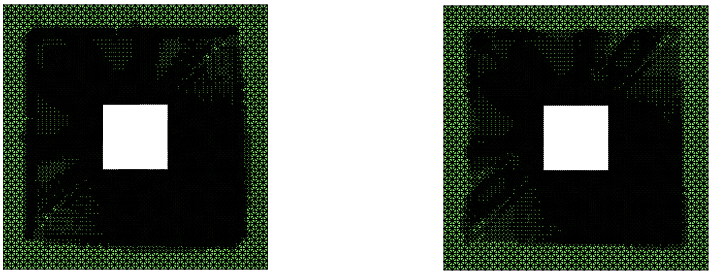

FIGURE 5.4. *The adaptive mesh with 16,509 nodes for the anisotropic PML method (left) and the adaptive mesh with 20,314 nodes for the uniaxial PML method (right) of Example 1. The condition number of the finite element stiffness matrix on the corresponding mesh is 5.6770e+04 for the anisotropic PML method and 1.1306e+06 for the uniaxial PML method.*

$k_2 = 8\pi$, $k_3 = 2\pi$. We also choose $L_1 = L_2 = 6$ and the thickness of PML layer $d_1 = d_2 = 1$. Figure 5.6 shows the setting of domain and the direction of the vector field along which the PML coordinate stretching is performed. We choose the PML parameters $\sigma_0 = 17.81$ and $r_0 = 0.5$ to ensure (5.22).

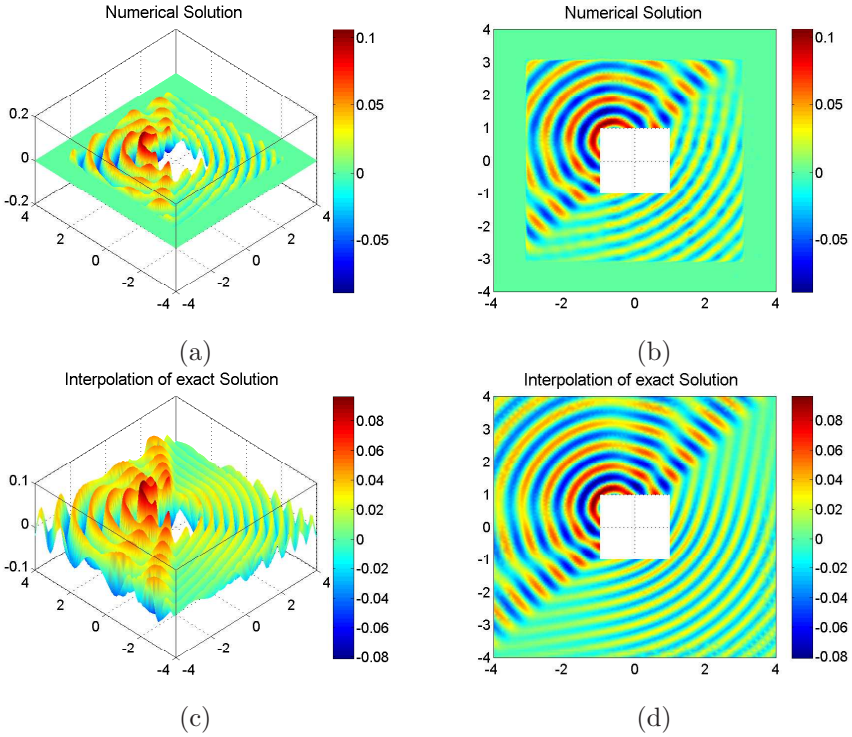


FIGURE 5.5. *Solutions of Example 1. (a) The numerical solution observed from the direction [-1,-1,2]; (b) The numerical solution observed from the direction [0,0,1]; (c) The exact solution observed from the direction [-1,-1,2]; (d) The exact solution observed from the direction [0,0,1].*

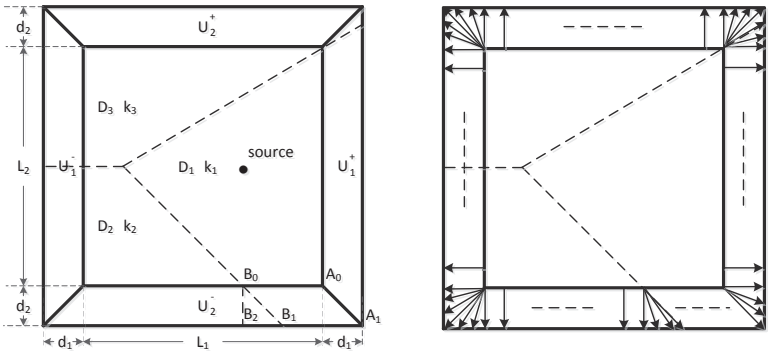


FIGURE 5.6. *The domain setting and the direction of the vector field along which the PML complex coordinate stretching is performed in Example 2.*

Now we describe the PML complex coordinate stretching transform $\tilde{x} = F(x)$ used in this example. Let $A_0 = (3, -3), A_1 = (4, -4), B_0 = (1, -3), B_1 = (2, -4)$,

and $B_2 = (1, -4)$ (see Fig. 5.6). The transform $F(x)$ is the same as the transform for the constant wave number in section 2 when $x \in \Omega_{\text{PML}} \setminus \bar{\Omega}_{A_0A_1B_2B_0}$, where $\Omega_{A_0A_1B_2B_0}$ denotes the quadrilateral with vertices $A_0, A_1, B_2, B_0$. To define the transform in $\Omega_{A_0A_1B_2B_0}$, we first notice that the distance between $A_0$, $B_0$ and the distance between $A_1$, $B_1$ satisfy $d_{A_0B_0} = d_{A_1B_1} = 2$. For $x \in \Omega_{A_0A_1B_2B_0}$, we define $r \in (0, \sqrt{d_1^2 + d_2^2}), s \in (0, 1)$ such that

$$\begin{aligned} x_1 &= \begin{cases} (\frac{L_1}{2} - s \cdot d_{A_0B_0}) + r\cos\theta & \text{if } x \in \Omega_{A_0A_1B_1B_0}, \\ (\frac{L_1}{2} - d_{A_0B_0}) + r\cos\theta \cdot s & \text{if } x \in \Omega_{B_0B_1B_2}, \end{cases} \\ x_2 &= -\frac{L_2}{2} - r\sin\theta. \end{aligned}$$

Here $\Omega_{A_0A_1B_1B_0}$ is the quadrilateral with vertices $A_0, A_1, B_1, B_0$ and $\Omega_{B_0B_1B_2}$ is the triangle with vertices $B_0, B_1, B_2$. Then the complex coordinate stretching function is

$$\begin{aligned} \tilde{x}_1 &= \begin{cases} (\frac{L_1}{2} - s \cdot d_{A_0B_0}) + \beta(r(x)) \left[x_1 - (\frac{L_1}{2} - s \cdot d_{A_0B_0})\right] & \text{if } x \in \Omega_{A_0A_1B_1B_0}, \\ (\frac{L_1}{2} - d_{A_0B_0}) + \beta(r(x)) \left[x_1 - (\frac{L_1}{2} - d_{A_0B_0})\right] & \text{if } x \in \Omega_{B_0B_1B_2}, \end{cases} \\ \tilde{x}_2 &= -\frac{L_2}{2} + \beta(r(x))(x_2 + \frac{L_2}{2}), \end{aligned}$$

where $r(x) = -\frac{L_2/2 + x_2}{\sin\theta}$.

Let the source $f$ be a Gaussian point source at $(r_1, r_2) = (1, 0)$

$$f(x) = e^{-(\frac{4k_1}{\pi})^2((x_1 - r_1)^2 + (x_2 - r_2)^2)}.$$

Figure 5.7 shows the adaptive mesh. We observe that the mesh in the domain with small wave number is coarser. Figure 5.8 shows the real part of numerical solution from two different observation directions. Figure 5.9 shows the log $N_k$-log $\mathcal{E}_k$ curve, where $N_k$ is the number of nodes of the mesh $\mathcal{M}_k$ and $\mathcal{E}_k$ is the associated a posteriori error estimate. It indicates clearly that the meshes and the associated numerical complexity are quasi-optimal: $\mathcal{E}_k \approx CN_k^{-1/2}$ is valid asymptotically.

## REFERENCES


[1] J.P. Bérenger, *A perfectly matched layer for the absorption of electromagnetic waves,* J. Comput. Phys., **114** (1994), 185-200.

[2] J.H. Bramble and J.E. Pasciak, *Analysis of a Cartesian PML approximation to acoustic scattering problems in* $\mathbb{R}^2$ *and* $\mathbb{R}^3$, J. Appl. Comput. Math., to appear.

[3] Z. Chen and H. Wu, *An adaptive finite element method with perfectly matched absorbing layers for the wave scattering by periodic structures* SIAM J. Nummer. Anal., **41** (2003), 799-826.

[4] Z. Chen and X. Liu, *An adaptive perfectly matched layer technique for time-harmonic scattering problems,* SIAM J. Numer. Anal., **41** (2003), 799-826.

[5] Z. Chen and X.M. Wu, *An adaptive uniaxial perfectly matched layer technique for time-Harmonic Scattering Problems*, Numerical Mathematics: Theory, Methods and Applications, **1** (2008), 113-137.

[6] J. Chen and Z. Chen, *An adaptive perfectly matched layer technique for 3-D time-harmonic electromagnetic scattering problems,* Math. Comp., **77** (2008), 673-698.

[7] Z. Chen and W. Zheng, *Convergence of the uniaxial perfectly matched layer method for time-harmonic scattering problems in two-layered media*, SIAM J. Numer. Anal., **48** (2010), 2158-2185.

[8] Z. Chen, T. Cui, L. Zhang, *An adaptive anisotropic perfectly matched layer method for 3D time harmonic electromagnetic scattering problems,* Numer. Math., to appear.

[9] W.C. Chew, *Waves and Fields in Inhomogeneous Media*, Springer, New York, 1990.

[10] W.C. Chew and W. Weedon, *A 3D perfectly matched medium from modified Maxwell's equations with stretched coordinates,* Microwave Opt. Tech. Lett., **7** (1994), 599-604.

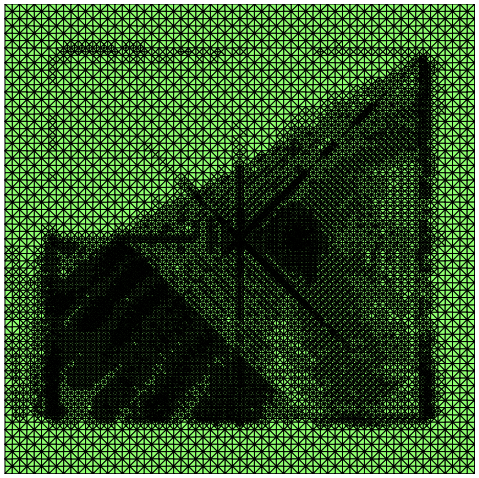

FIGURE 5.7. *The adaptive mesh with 16,137 nodes of Example 2.*

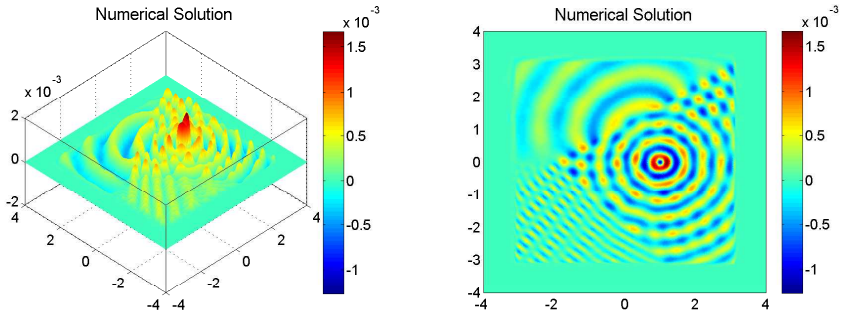


(a) (b)

FIGURE 5.8. *Solutions of Example 2. (a) The numerical solution observed from the direction [-1,-1,2]; (b) The numerical solution observed from the direction [0,0,1].*

[11] F. Collino and P.B. Monk, *The perfectly matched layer in curvilinear coordinates*, SIAM J. Sci. Comput., **19** (1998), 2061-2090.
[12] T. Hohage, F. Schmidt, and L. Zschiedrich, *Solving time-harmonic scattering problems based on the pole condition. II: Convergence of the PML method*, SIAM J. Math. Anal., **35** (2003), 547-560.
[13] S. Kim and J.E. Pasciak, *Analysis of a Cartisian PML approximation to acoustic scattering problems in* $\mathbb{R}^2$, J. Math. Anal. Appl., **370** (2010), 168-186.
[14] M. Lassas and E. Somersalo, *On the existence and convergence of the solution of PML equations*, Computing, **60** (1998), 229-241.
[15] M. Lassas and E. Somersalo, *Analysis of the PML equations in general convex geometry*, Proc. Roy. Soc. Eding., **131** (2001), 1183-1207.

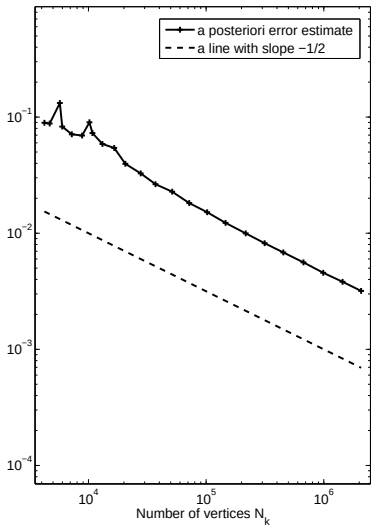


FIGURE 5.9. *The quasi-optimality of the adaptive mesh refinements of the a posteriori error estimate for Example 2.*

[16] K.C. Meza-Fajardo and A.S. Papageorgiou, *A nonconventional, split-field, perfectly matched layer for wave propagation in isotropic and anisotropic elastic media: stability analysis,* Bulletin Seismological Soc. Am., **98** (2008), 1811-1836.

[17] A.F. Oskooi, L. Zhang, Y. Avniel, and S.G. Johnson, *The failure of perfectly matched layers, and towards their redemption by adiabatic absorbers,* Optical Express, **16** (2008), 11376-11392.

[18] F.L. Teixeira and W.C. Chew, *Advances in the theory of perfectly matched layers,* In: "Fast and Efficient Algorithms in Computational Electromagnetics" (eds W.C. Chew et al), Artech House, (2001), 283-346.

[19] D.V. Trenev, *Spatial Scaling for the Numerical Approximation of Problems on Unbounded Domains*, PhD Thesis, Texas A& M University, 2009.

[20] E. Turkel and A. Yefet, *Absorbing PML boundary layers for wave-like equations*, Appl. Numer. Math., **27** (1998), 533-557.

[21] L. Zschiedrich, R. Klose, A. Schödle, and F. Schmidt, *A new finite element realization of the perfectly matched layer method for Helmholtz scattering problems on polygonal domains in two dimensions,* J. Comput. Appl. Math., **188** (2006), 12-32.

*E-mail address*: zmchen@lsec.cc.ac.cn
*E-mail address*: liangchao@lsec.cc.ac.cn
*E-mail address*: xiangxs@lsec.cc.ac.cn